

# Ecological Restoration from Space: The use of Remote Sensing for Monitoring Land Reclamation in Sudbury

Catherine M. Champagne<sup>1</sup>  
Abdelgadir Abuelgasim<sup>2</sup>  
Karl Staenz<sup>2</sup>  
Stephen Monet<sup>3</sup>  
H. Peter White<sup>2</sup>

## Abstract

The use of spatial information systems has grown over the past decade as a tool for studying ecosystems and the impacts of human activity upon them. The collection of geographic data, however, is often time consuming and expensive. Remote sensing of ecological processes offers the potential to rapidly produce spatial information over large areas. This study will examine the use of earth-observation data to map the restoration activities in the City of Greater Sudbury. Sudbury has made great progress over the past 25 years in restoring the vegetation cover that had been destroyed by the effects of mining. Reductions in smelter emissions and a reclamation effort to re-vegetate the area through a large-scale soil liming and tree-planting campaign have resulted in significant land cover change. Preliminary results show that remote sensing data can produce information on the land cover type and, on the relative health of vegetation in restored areas that are consistent with other field-based studies in this region. Further validation of these results need to be made to determine the local accuracy level that can be achieved using these methods.

## Introduction

Sustainable development has become an important priority of the mining sector over the past decade. The environmental impacts of mining are significant ranging from habitat disturbance due to mine development, to the impact of acid-generating tailings, to the effects of airborne pollution from smelting activities.

<sup>1</sup> Mir Télédétection inc, Longueuil, QC, Canada J4K-1A3

<sup>2</sup> Canada Centre for Remote Sensing, Earth Sciences Sector, Natural Resources Canada, Ottawa, ON, Canada

<sup>3</sup> City of Greater Sudbury, Sudbury, ON, Canada

Improvements in emissions controls from metal smelters, as well as stricter legislation for mine operation and closure have reduced these environmental impacts. Communities with a history of mining activities, however, are faced with the difficult task of restoring areas with significant ecological disturbance. Planning ecological restoration activities, and monitoring the results of these activities can be time consuming and expensive relying on field measurements alone. Remote sensing technology offers a potential non-intrusive solution to provide biogeospatial information over large regions. These data sets could complement more detailed field-evaluation data and provide baseline information to permit long-term monitoring of restored sites.

Satellite remote sensing for environmental applications has been in use for several decades. As sensor technology improves, and methods to correct and extract information from these types of data are further developed and validated, this technology becomes a more reliable means of evaluating ecological processes. This paper will discuss the potential application of remote sensing and geographic information systems (GIS) to ecological restoration of mining-impacted areas, within the context of the Sudbury Regional Land Reclamation Program. Preliminary results of analyses performed on data collected in 2003 are presented, and plans for future work in this area will be outlined.

## Ecological Restoration in Sudbury

The Sudbury region is renowned for its rich mineral deposits that have formed the basis of the mining industry in the region for over 100 years. The city lies on a precambrian bedrock rich in iron-sulphides that contains one of the largest known deposits of nickel-copper-platinum group elements in the world. Historically, this region was characterized by stands of white and red pine mixed with tolerant hardwood species. Nickel mining and metal extraction activities began in the area in the 1880's. Initially, open-bed roast yards were used to refine the ore, a process that involved piling crushed ore on top of firewood and allowing the ore to burn for several months. This produced significant emissions of sulphur-dioxide that left localized areas barren. In the 1930's, this process was replaced by metal smelting, where the ore was ignited in a contained furnace, and the emissions was distributed through smokestacks. These emissions contained both sulphur dioxide copper and nickel particles, which led to a long-term poisoning of the surrounding soils and left an impact on an area as large as 5600 km<sup>2</sup> (Winterhalder, 2002).

Improvements in emissions reductions and ore processing technologies in the 1970's created the potential to restore the areas left barren or significantly denuded of vegetation. Beginning in 1979, barren

regions were limed to reduce soil acidity and immobilize metal contaminants. This was followed by fertilizer application, and the planting of mixed grasses. Grassing was followed by the planting of trees and shrubs, primarily species of pine (*Pinus resinosa*, *P. strobus*, *P. banksinana*). Natural re-colonization has occurred on many of these areas as soil and atmospheric conditions have improved, primarily white birch (*Betula papyrifera*) and trembling aspen (*Populus tremuloides*). The restoration program continues, with an increasing focus on restoring the vegetation cover for both aesthetic reasons and to improve biodiversity and wildlife habitat. The process of recovery will be slow, and the composition of the resulting ecosystem uncertain (Winterhalder, 2002). The long-term, dynamic nature of this process makes the availability of cost-effective monitoring tools an essential element of evaluating its progress.

## Ecological Applications of Remote Sensing

Remote sensing data are collected for ecological applications in two broad categories: passive and active sensors. Passive sensors measure radiation reflected (in the optical domain) or emitted (in the thermal or microwave domain) from the earth's surface. Active sensors send out electromagnetic pulses to the surface, and measure the returned signal. The most common active sensors are synthetic aperture radar, which operate in the microwave range. Radar sensors have been used for applications related to wetland classification (Sokol *et al*, 2000), biomass estimation

(Moreau and Le Toan, 2003) and hydrological modelling (Deshamps *et al*, 2002). Optical sensors measure reflected solar radiation from the earth's surface, which has been used to evaluate vegetation species composition, vegetation carbon uptake and vegetation stress (Chen *et al*, 2003; Underwood *et al*, 2003; Champagne *et al*, 2003).

Optical sensors can be sub-categorized according to the number of spectral bands for which they collect information. Multispectral sensors, such as Landsat TM, measure reflected radiation in a series of discrete and broad spectral bands. Hyperspectral sensors, such as the Airborne Visible/Infrared Imaging Spectrometer (AVIRIS) and the Compact Airborne Spectrographic Imager (*casi*), usually have 50 or more narrow spectral bands, to produce a contiguous spectral signature for each ground pixel (Fig. 1). There are advantages to using both types of information for evaluating the success of ecological restoration efforts. Multispectral sensors often cover a much larger geographic area, allowing for assessment of regional patterns in land cover change. In addition, satellite-borne multispectral sensors have been in use for a longer period of time, and archived historical data exists for many areas. Conversely, hyperspectral sensors are a relatively new technology, and have traditionally been used on airborne platforms, resulting in limited historical data that was often collected over small geographic areas for dedicated campaigns. Due to the high spectral resolution of hyperspectral sensors, quantitative ground parameters can be derived, such as vegetation cover, leaf area index (LAI), canopy liquid water (LW) and chlorophyll (Levesque *et al*, 1997; McNairn *et al*, 2001; Champagne *et al*, 2003). New hyperspectral satellite-borne sensors are currently in operation, and the development of new sensors is ongoing (Staenz and Hollinger, 2003). Limited field-scale validation of ecological parameters derived from hyperspectral data has been made in the past, and more rigorous testing of biophysical and biochemical parameter extraction methods needs to be explored for this technology to be used operationally for ecological restoration applications. Also, the scaling of algorithms developed for airborne sensors to the more coarse resolution of satellite sensors is an ongoing research issue.

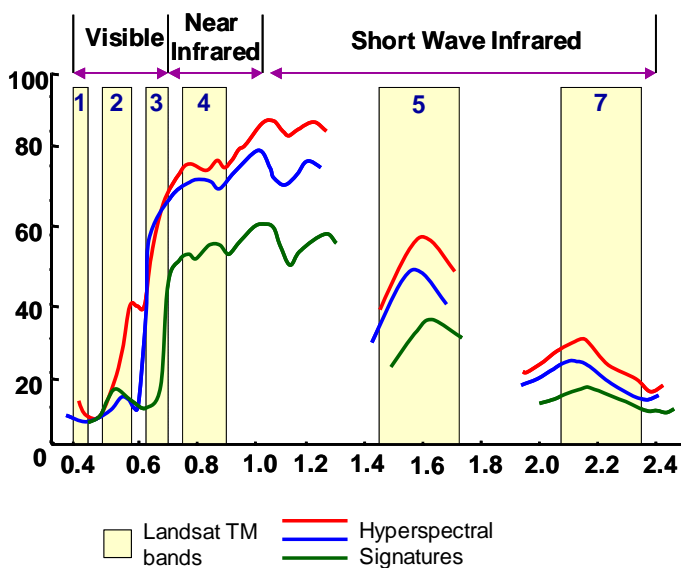


Figure 1. Comparison of spectral information available in multispectral (Landsat TM bands, shown in yellow bars) and hyperspectral (spectral signatures of vegetation shown in red, green and blue) remote sensing data.

## Data and Methods

### Image Data

Image data were acquired from two satellite-borne optical sensors in the summer of 2003. A Landsat 5 multi-spectral image was acquired over the Sudbury region on June 25, 2003. Landsat 5 has seven spectral bands in the visible and near infrared (VNIR) and short wave infrared (SWIR), and one band in the thermal region of the electromagnetic spectrum. Each spectral

band has a nominal spatial resolution of 30 by 30 m on the ground. An EO-1 Hyperion image was acquired on August 13, 2003 along a north-south transect centered over the Copper Cliff tailings and smelter site within the Sudbury region. Hyperion has 242 contiguous spectral bands in the VNIR and SWIR, covering wavelengths from 400 to 2500 nm in the electromagnetic spectrum, each with a spatial resolution of 30 m by 30 m. The sensor parameters for both data sets are given in Table 1.

	Landsat 5	Hyperion
Acquisition Date	June 25, 2003	August 10, 2003
Spectral Coverage	450 - 2350 nm	400 – 2500 nm
Number of Bands	7	242
Band Width	60 - 270 nm	8 - 14 nm
Spatial Resolution (optical bands)	30 m	30 m
Swath Width	185 km	7.7 km

Table 1. Sensor characteristics for remote sensing data.

### Image Processing

The Landsat 5 imagery was received corrected for systematic sensor distortions and calibrated to at-sensor radiance. The image was also corrected for geometric distortion caused by variation in the sensor, the satellite platform and earth curvature and rotation. The data was processed to at-surface reflectance using the Imaging Spectrometer Data Analysis System (ISDAS; Staenz *et al.*, 1998). The corrected image was classified using an unsupervised clustering algorithm (K-means) in PCI software. K-means was first applied with 16 clusters and these were further reduced to 14 labelled classes, based on interpretation using field measurements and aerial photography.

The Hyperion data pre-processing was done using a series of algorithms available in the ISDAS software (White *et al.*, 2004). The image was initially corrected for errors in detector alignment and vertical banding was removed using an automated technique. Sensor noise was reduced using an automated technique that models sensor noise based on each detector's characteristics and removes the noise by comparing neighboring spectral bands in the along-track direction. Calibration errors were modelled and corrected using a sensor "smile" detection and correction algorithm that included correction to gain/offset errors (Neville *et al.*, 2003). The effects of atmospheric scattering by gas molecules and aerosols were removed by calibrating the image to surface reflectance using the MODTRAN 4.2 atmospheric transmission code, utilizing a semi-empirical model to estimate column atmospheric water vapour (Staenz and Williams, 1997). Several parameters

were derived from the corrected Hyperion image. The canopy liquid water content was estimated simultaneous to water vapour estimation (Staenz *et al.*, 1997). Canopy liquid water content can be used as a means of evaluating the health of vegetation stands, due to its relationship to biophysical parameters such as LAI (Roberts *et al.*, 1998). Finally, forest canopy closure was estimated using a weakly-constrained, linear spectral-unmixing routine in ISDAS. This method classifies each image pixel into a series of fractions, based on the similarities of pixel spectra to "pure" reference spectra of each ground element. For this analysis, reference spectra were selected from the image scene based on knowledge of the area, to approximate fractions of dense pine vegetation, water, bare soil, and mine waste. LW and percent cover maps were masked to remove data from zones classed as urban, industrial and water from the Landsat data. This was done to limit the analysis to zones that have the potential to be reclaimed.

All image products were georeferenced using an image-to-image registration with orthorectified Landsat data from the Canadian Centre for Topographic Information (Natural Resources Canada, 2004). Errors in geometric registration were less than the spatial resolution of the scenes, with a root mean squared error of 0.2 pixels for the Landsat and 0.7 pixels for the Hyperion.

### Field Data

Field measurements were made concurrent to the acquisition of Hyperion data in August of 2003. Twelve 10 by 10 metre plots were selected randomly in forested areas within the swath of the Hyperion sensor. In each plot, the number of trees and species were recorded. These were used to assign forest species classes to the result of the unsupervised image classification.

Additional field measurements were obtained from the City of Greater Sudbury's restoration planning database. Digital polygons outlining areas that were restored under the Sudbury Land Reclamation Program since 1979 were used to evaluate the effectiveness of remote sensing tools for monitoring managed ecological restoration in the area. The database included information on the number and species of trees and other vegetation planted in each plot, and the years when planting was done. A subset of 60 reclamation polygons that fell within the swath of the Hyperion imagery was used for the current analysis.

To augment this analysis, information was also extracted from polygons representing impact zones around the smelter site, representing distances of 3 km, 8 km, 30 km and 60 km. The first three zones were selected based on the approximations of Ripley, *et al.* (1996). The area within 3 km of the emissions sites represented areas where no tree canopy was present in the 1970's. Within 8 km of the smelters, forest cover

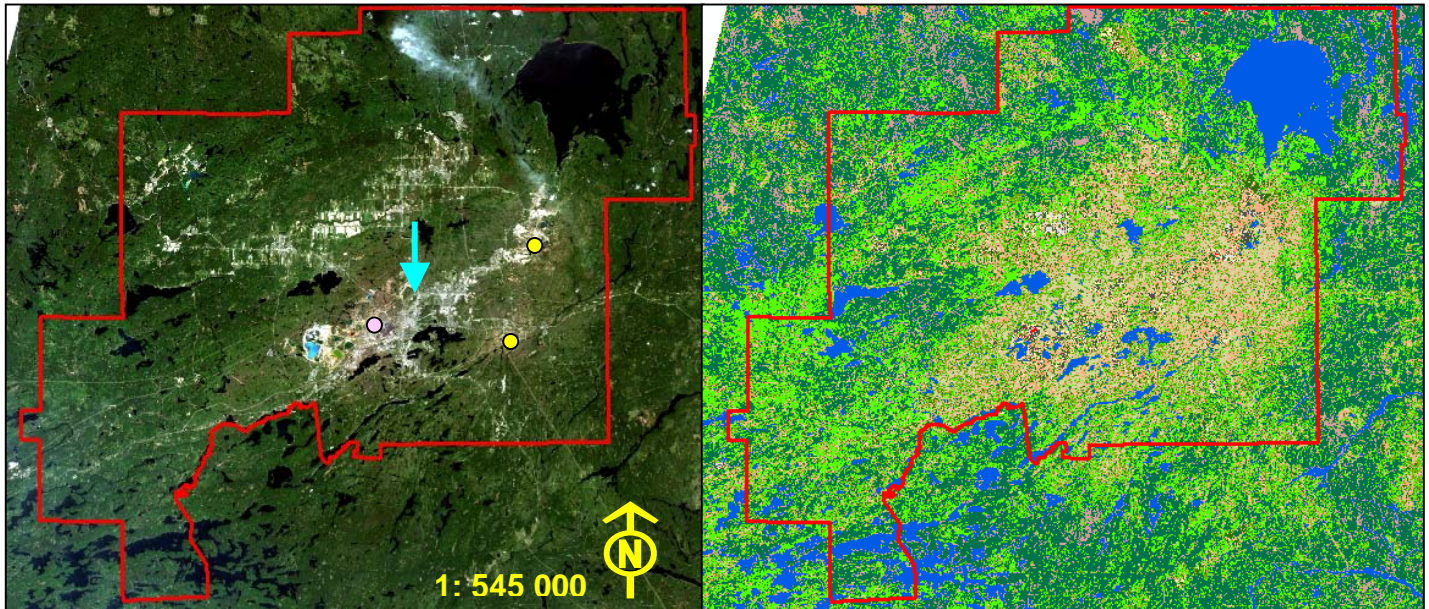
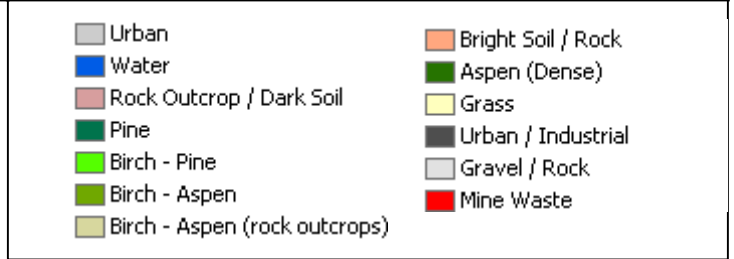


Figure 2. Left: False-colour image from Landsat over City of Greater Sudbury (approximate border outlined in red) with the location of the Copper Cliff smelter indicated with a rose-coloured point and other historical metal smelters indicated with yellow points; the approximate location of the urban core indicated with a blue arrow; Right: Results of the unsupervised land cover classification of Landsat imagery)



was limited to valleys. Within 30 km, the vegetation canopy was below regional norms of species richness. A zone representing the 30 km to 60 km area away from the smelter was also selected to compare impacted zones to areas where reduced impact has been observed, based on soil and atmospheric measurements (Ripley *et al.*, 1996). All image data products were integrated in a GIS, and statistics were extracted from both the impact zone polygons and the polygons defined by the Reclamation program.

### Results and Discussion

The results of the land cover classification of Landsat data are given in Figure 2. The area consists of an urban core (approximately in the centre of the image), an agricultural region to the north-east of the urban core, and a large area surrounding the city consisting of lakes and forest cover. The classification results show a general pattern of Birch-Aspen tree assemblages near the urban core and around the smelter sites, with a trend towards increased Pine and Pine-Birch classes away from the urban / industrialized area.

The distribution of land cover classes in each impact zone is given in Figure 3. The zone closest to the smelter has a high percentage of land area falling in the Rock / Dark soil class, and the portion of the cover type gradually diminishes with distance away from the

smelter. Also notable is the decline in the Birch-Aspen-Rock-Outcrop class with distance from the smelter. This is consistent with results obtained by Courtin (1998), who observed the dominance of coppiced birch woodlands in the transitional vegetation zones around the smelter sites. These zones were largely composed of widely spaced birch, that were small in size, with large canopy gaps. Limited validation data was available for this preliminary analysis, but future work will involve the collection of more detailed ground information, and the refinement of methodologies to best derive land cover information.

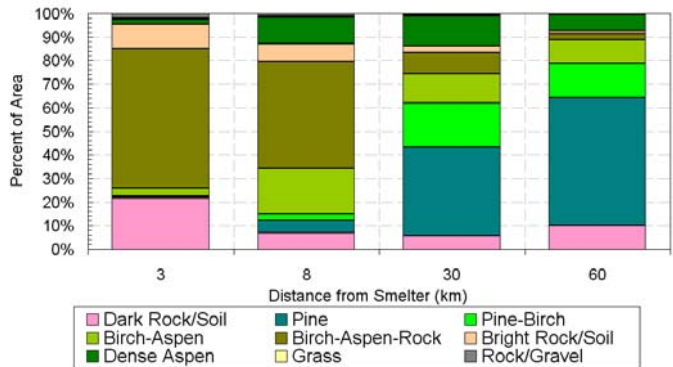


Figure 3. Frequency of land cover classes in impact zones around the Copper Cliff smelter site (expressed as a percentage of the total area). Urban, industrial and water classes have been excluded from the analysis.

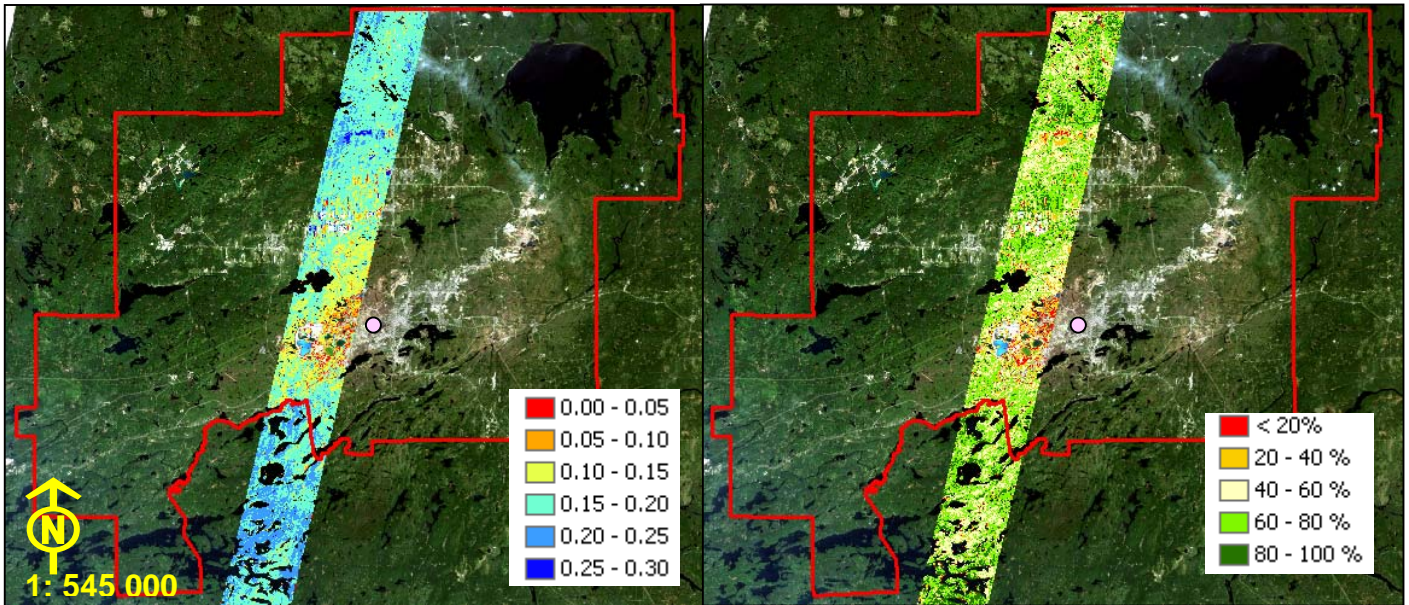


Figure 4. Left: Classified image of vegetation liquid water content (LW) derived from Hyperion data (with Landsat false-colour image in background). LW values are in  $\text{g cm}^{-2}$ . Right: Classified image of canopy percent cover derived from Hyperion data. The location of the smelter is indicated with a rose-coloured point.

The maps of canopy LW and vegetation percent cover are given in Figure 4. The overall pattern indicates that areas closest to the smelter have vegetation canopies with lower water content ( $0.09 \text{ g cm}^{-2}$  within 3 km versus  $0.18 \text{ g cm}^{-2}$  from 30 – 60 km), an indication that the vegetation in these areas is less vibrant, with fewer leaves and therefore less photosynthetic surface area. The vegetation becomes more vibrant in areas further away from the smelter, particularly in areas to the southwest, which could be indicative of the predominant direction of prevailing winds. Similarly, the percent cover map shows values less than 50% in the area closest to the smelter site (21.8 % cover within 3 km and 45.7 % cover from 3 – 8 km), and a trend toward fuller vegetation canopies at increased distance (62.7% cover in the 8 – 30 km zone and 65.2% cover in the 30 – 60

km zone). The average values of both liquid water and percent cover show a similar pattern in the defined impact zones around the smelter site (Fig. 5). These two measures of vegetation health were not correlated on an individual pixel basis ( $r = 0.2$ ). The areas within 3km and 8km, that had been observed to be all but barren of vegetation in the 1970's, show some sparse vegetation,

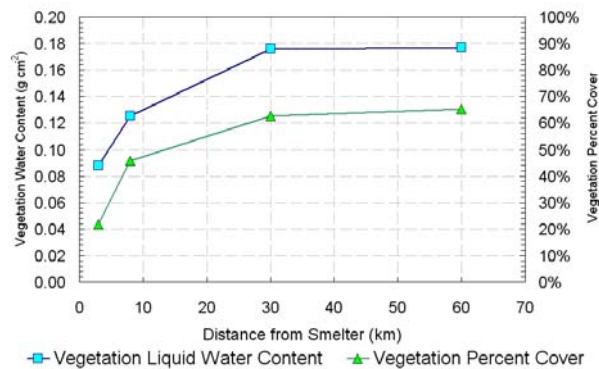


Figure 5. Average values of vegetation liquid water (LW) and vegetation percent cover within impact zones around the Copper Cliff smelter.

	<i>Mean</i>	<i>Min</i>	<i>Max</i>	<i>Standard Deviation</i>
Liquid Water Content ( $\text{g cm}^{-2}$ )	0.12	0.04	0.17	0.02
Vegetation Percent Cover	48.70%	0.37%	68.05%	12.33%
<b>Vegetation Classes (Areal Coverage)</b>				
Rock Outcrop / Dark Soil	4.5%	0.0%	31.4%	7.0%
Pine	4.5%	0.0%	31.4%	7.0%
Pine - Birch	3.9%	0.0%	33.2%	7.0%
Birch - Aspen	17.6%	0.0%	51.5%	14.5%
Birch - Aspen (rock outcrops)	51.4%	0.0%	100.0%	32.9%
Bright Soil / Rock	4.5%	0.0%	53.2%	9.1%
Aspen	13.1%	0.0%	50.0%	13.9%
Grass	0.5%	0.0%	20.5%	2.7%

Table 2. Summary statistics for reclamation polygons.

the areas that were less impacted beyond the 30km distance from the smelter, show a relatively consistent vegetation pattern (higher LW, vegetation cover in the 60 – 70% range). On a regional scale, these observations agree with the restoration patterns that have been observed in this area (Courtin, 1995; Anand, 2004).

Information on land cover type and vegetation health were extracted from the image data for each of the reclamation polygons in the scene (Table 2). Of the 60 polygons chosen, 39 fell within 3 – 8 km of the smelter site, with the remaining 21 falling in the 8 - 30 km zone. The dominant land cover type for most of the polygons was the Birch-Aspen-Rock-Outcrop class, covering 51.4 % ( $\pm 32.9\%$ ) of the land area on average (Table 2). The Birch-Aspen and Aspen classes were also relatively common with average values of 17.6 ( $\pm 14.5\%$ ) and 13.1 % ( $\pm 13.9\%$ ), respectively. This suggests that a great deal of natural colonization has occurred within these zones, since many of the dominant tree species are deciduous and the planted species were primarily coniferous. Further investigation will need to be made to determine the local accuracy of these results using field measurements.

The vegetation health measurements for the reclamation polygons show average values of 0.12 ( $\pm 0.02$ )  $\text{g}\cdot\text{cm}^{-2}$  for vegetation liquid water content and 48.7% ( $\pm 12.33\%$ ) for vegetation cover. The overall values were slightly higher for polygons further away from the smelter site (0.18  $\text{g}\cdot\text{cm}^{-2}$  versus 0.12  $\text{g}\cdot\text{cm}^{-2}$  of canopy liquid water for reclamation polygons within the 8km and 30km zones, respectively; 62.7% and 45.7% vegetation cover for reclamation polygons within the 30km and 8km zones, respectively). This could suggest that residual contamination in the soil may be playing a role in reducing the vitality of vegetation in the reclamation polygons. This will be investigated further in future research.

## Conclusions and Future Prospects

The use of multiple sources of optical remote sensing was explored for use in evaluating the success of reclamation efforts in the Sudbury area. A land cover map was derived from Landsat data collected in 2003 and vegetation health parameters were extracted from Hyperion hyperspectral imagery collected in 2003. The land cover information extracted from Landsat showed a trend towards coniferous forests at distance from the historical smelter emission source. The vegetation health parameters extracted from Hyperion showed a trend towards higher liquid water content in trees away from the source (0.09  $\text{g}\cdot\text{cm}^{-2}$  within 3 km versus 0.18  $\text{g}\cdot\text{cm}^{-2}$  from 30 – 60 km), indicating greater photosynthetic capacity, and overall health of trees away from the emissions source. The areas closest to the smelter showed more sparse vegetation canopies (21.8 % cover within 3 km versus 65.2 % cover from 30 – 60 km).

These results are consistent with patterns observed by other field-based studies in this region.

Preliminary results from the subset of areas that were reclaimed through the Regional Reclamation Program show that there is a moderate vegetation cover in these areas (48.7%  $\pm 12.33\%$ ) and the photosynthetic vitality of the trees remains moderate (0.12  $\pm 0.02$   $\text{g}\cdot\text{cm}^{-2}$ ) for vegetation liquid water content. These areas are predominantly covered in a Birch-Aspen canopy with significant rock outcrops. This analysis will be expanded to include a greater number of reclamation polygons and will include ground validation to determine the accuracy of these results.

Overall, the use of integrated remote sensing and geographic information systems to evaluate success in ecological restoration is promising. Further work is needed to determine the accuracy of image-derived vegetation parameters, and to improve methods to derive land cover information. Future work will examine this, and explore the potential for modelling reclamation scenarios using spatial information systems.

## Acknowledgements

This research is part of the Earth Sciences Sector's Sustainable Development Through Knowledge Integration Program at Natural Resources Canada. The authors would like to acknowledge L. Sun for assistance with image processing and R. Neville and J. Shang and M. Beauchemin for assistance and comments on the research. The authors also acknowledge the support of the Sudbury Regional Reclamation Program for providing data for the analysis.

## References

- Anand, M. and R.E. Desrochers. 2004. Quantification of restoration success using complex systems concepts and models. *Restoration Ecology*, 12: 117-123.
- Champagne, C., K. Staenz, A. Bannari, H. McNairn, and J-C. Deguise. 2003. Validation of a hyperspectral curve-fitting model for the estimation of plant water content in agricultural canopies. *Remote Sensing of Environment*, 87:148-160.
- Chen J. M., J. Liu, S.G. Leblanc, R. Lacaze, and J-L. Roujean. 2003. Multi-angular optical remote sensing for assessing vegetation structure and carbon absorption. *Remote Sensing of Environment*, 84 (4): 516-525.
- Courtin, G.M. 1995. Birch Coppice Woodlands near the Sudbury Smelters: Dynamics of a Forest Monoculture. Pages 299-312 in J.M. Gunn, editor. *Environmental restoration and recovery of an industrial region*. Springer-Verlag, New York, NY.

- Deschamps A., D. Greenlee, T.J. Pultz, R. Saper. 2002. Geospatial data integration for applications in flood prediction and management in the Red River basin. International Geoscience and Remote Sensing Symposium, Toronto, Canada.
- Lévesque, J., T. Szeredi,, K. Staenz, V. Singhroy, and D. Bolton. 1997. Spectral unmixing for monitoring mine tailings site rehabilitation, Copper Cliff mine, Sudbury, Ontario. In Proceedings of the Twelfth International Conference and Workshops on Applied Geological Remote Sensing, Denver, Colorado.
- McNairn H., J-C. Deguise, A. Pacheco, J. Shang, N. Rabe. 2001. Estimation of crop cover and chlorophyll from hyperspectral remote sensing; Proceedings of the 23rd Canadian Symposium on Remote Sensing, Ste. Foy, Quebec.
- Moreau, S. and T. Le Toan. 2003. Biomass quantification of Andean wetland forages using ERS satellite SAR data for optimizing livestock management. Remote Sensing of Environment, 84 (4) : 477-492.
- Natural Resources Canada. 2004. Landsat 7 Orthorectified Imagery Over Canada. <http://geogratis.cgdi.gc.ca>.
- Neville, R. A., L. Sun, and K. Staenz. 2003. Detection of spectral line curvature in imaging spectrometer data. Proceedings of SPIE on Algorithms and Technologies for Multispectral, Hyperspectral, and Ultraspectral Imagery IX, SPIE 5093: 144-154.
- Ripley, E.A., and R.E. Redham, A.A. Crowder. 1996. The Environmental Effects of Mining. St. Lucie Press, Delray Beach, Fla.
- Roberts, D.A., K. Brown, R. Green, S. Ustin, and T. Hinckley. 1998. Investigating the relationship between liquid water and leaf area in clonal populus. Summaries of the Seventh JPL Earth Science Workshop, Pasadena, CA.
- Sokol J., T.J. Pultz, V. Bulzgis. 2000. Monitoring wetland hydrology in Atlantic Canada using multi-temporal and multi-beam RADARSAT data. Remote Sensing and Hydrology 2000, Santa Fe, New Mexico.
- Staenz, K., T. Szeredi, R.J. Brown, H. McNairn, and R. Van Acker. 1997. Hyperspectral information extraction techniques applied to agricultural data for detection of within field variations. International Symposium, Geomatics in the Era of RADARSAT (GER'97), Ottawa, Canada.
- Staenz, K., and D.J. Williams. 1997. Retrieval of surface reflectance from hyperspectral data using a look-up table approach. Canadian Journal of Remote Sensing, 23(4):354-368.
- Staenz, K., T. Szeredi, and J. Schwarz. 1998. ISDAS- A system for processing/analyzing hyperspectral data. Canadian Journal of Remote Sensing, 42(2): 99-113.
- Staenz, K., and A.H. Hollinger, 2003, A Canadian hyperspectral spaceborne mission - applications and user requirements. Proceedings of the 3rd EARSeL Workshop on Imaging Spectroscopy, Oberpfaffenhofen, Germany.
- Underwood, E., S.L. Ustin and D. DiPietro. 2003. Mapping nonnative plants using hyperspectral imagery. Remote Sensing of Environment, 86:150 – 161.
- Winterhalder, K. 2002. The effects of the mining and smelting industry on Sudbury's landscape, in The Physical Environment of the City of Greater Sudbury, ed. D.H. Rousell and K.J. Jansons, OGS Special Volume 6, p145-174.
- White, H.P., S.K. Khurshid, R. Hitchcock, R. Neville and L. Sun., C.M. Champagne and K. Staenz. 2004. From at-sensor observation to at-surface reflectance – calibration steps for earth observation hyperspectral sensors, Proceedings of IGARSS 2004, Anchorage, U.S., September 20-24.